

Transverse Strain Response of Silicone Dielectric Elastomer Actuators

G. Yang, W. Ren, B.K. Mukherjee, G. Akhras
Centre for Smart Materials and Structures, Royal Military College of Canada,
Kingston, Ontario, Canada

J.P. Szabo
Defence Research and Development Canada Atlantic, Dartmouth, Nova Scotia, Canada

ABSTRACT

A strain measurement system based on the Zygo Doppler laser interferometer has been used to study the static and dynamic transverse strain response of Maxwell stress actuators made from Dow Corning HSIII silicone films over a wide displacement range and at frequencies from DC to 100 Hz. The time dependence of the strain response has been investigated. The effect of a mechanical tensile pre-load or pre-strain on the transverse strain has been studied. There is an initial increase in the strain due to pre-load but the transverse strains decrease when larger pre-loads are applied. Geometric effects are shown to be important and models of hyperelasticity that are capable of describing the large deformations of polymer materials have been used to interpret our results. A finite element simulation using a hyperelastic model provides good agreement with most of our observations on the electric field and pre-load dependencies of the transverse strain.

Keywords: dielectric elastomer actuator, Maxwell stress actuators, transverse strain, hyperelastic model, finite element analysis.

1. INTRODUCTION

Some electroactive polymers have been shown to have very large electric field-induced strains and their characteristics make them promising materials for many electromechanical actuator, transducer and active vibration damping applications.^{1,2} The characterisation of the dynamic strain response, especially under high driving fields, is difficult. Contact methods of strain measurement are generally unsuitable as the contacts often cause mechanical clamping and reduce the strain of the soft polymer materials. Non-contact methods used include optical microscopy³ the low resolution of which makes small strain measurements difficult, and cantilever beam based dilatometry with a photonic sensor⁴ that cannot, however, measure large displacements.

We have used a Zygo ZMI 2000 laser Doppler interferometer to measure transverse strains in Maxwell stress actuators fabricated from Dow Corning HSIII Silicone films⁵. The system uses a heterodyne detection technique and features a wide bandwidth, high stability, easy optical alignment and the ability to measure a wide range of displacements, from 0.62 nm to 21.2 m, at frequencies from DC up to 100 Hz. The static and dynamic strains of the materials have been measured as functions of amplitude and frequency under various types of driving electric fields such as a step field, an AC field and a DC bias field. In addition, the effect of a mechanical tensile pre-load on the transverse strain has also been investigated. The large deformations in these materials can only be understood using models of hyperelasticity. Finite element modelling of the elastomers has been carried out using ANSYS with a hyperelastic model and the results provide good agreement with most of our observations.

2. EXPERIMENT

Figure 1 shows a transverse strain measurement system based on the Zygo laser Doppler interferometer (ZMI 2000, Zygo Corp.). The top part of the polymer film is clamped on a fixed sample holder whereas its bottom end is attached to a very light platform that moves with the sample. A reflecting mirror on the platform reflects the measuring laser beam. The platform weighs about 18 grams and acts as a preload on the polymer film.

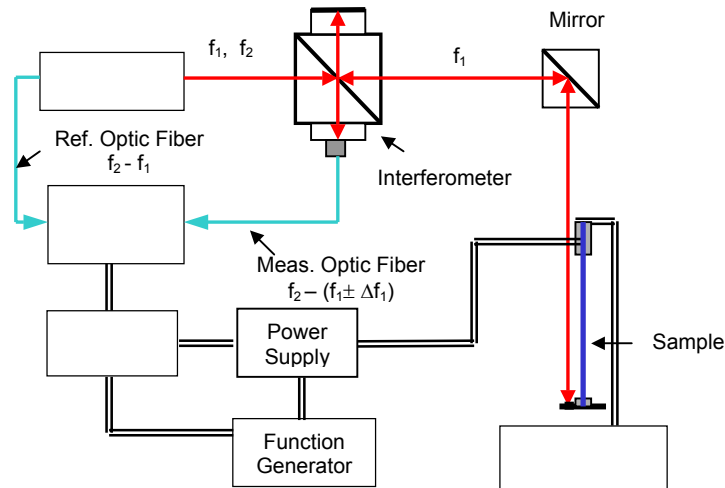


Figure 1. Schematic of transverse strain measurement system based on the Zygo laser Doppler interferometer

For the investigation of the effect of mechanical load, we hung additional metal blocks of different weights on the platform. The platform is adjusted so that the surface of the mirror is perpendicular to the polymer surface and the reflected laser beam has the same optical pathway as the incident beam, which results in the maximum output signal. The elongation of the polymer film produced by an electric field causes the bottom end of the sample to move and this movement is detected by the laser interferometer via the mirror on the platform. The transverse (vertical) strain of the polymer is provided by the Doppler interferometer. A computer using NI-VME interfaces controls the measuring system. A selected waveform voltage generated by a HP33120A function generator is amplified by a Trek 20/20A power amplifier and then applied to the polymer film via the top sample holder. Given the sensitivity of the laser interferometer to thermal and mechanical vibrations, the system was mounted on a floating optical bench with redundant vibration dampers. The sample geometry is shown in Figure 2. The usual dimensions of the polymer films and graphite electrodes were 70 mm × 150 mm and 50 mm × 80 mm respectively. The thicknesses of the polymer films varied from 80 μm to 260 μm. The static and dynamic strains of the polymer film actuators were measured as functions of amplitude and frequency under various driving electric fields. The dielectric properties of the polymer films were measured by a Solartron 1260 impedance analyzer via a Solartron 1296 dielectric interface at 1 V (rms value) over the frequency range from 0.01 Hz to 100 kHz.

3. EXPERIMENTAL RESULTS

Figure 3 shows the time dependence of the transverse elongation of HS III silicone film under a step voltage of 2.4 kV. There are clearly two parts to the response: the fast part of the responses accounts for about 75% of the total measured strain and the slow part takes about 10 seconds to reach up to 90% of the total measured

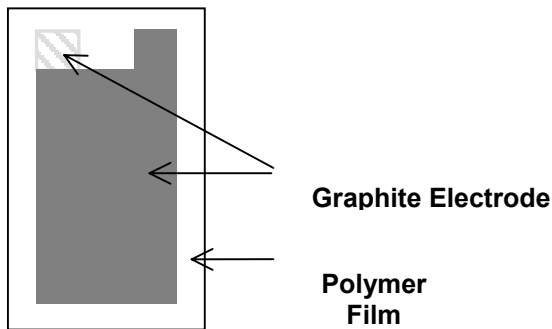


Figure 2. Schematic of the polymer film

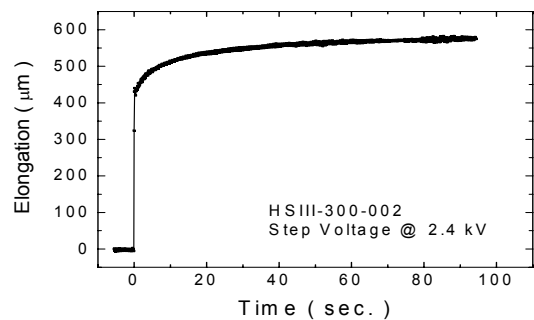


Figure 3. Transverse elongation of HS III silicone polymer film as a function of time under a step electric field.

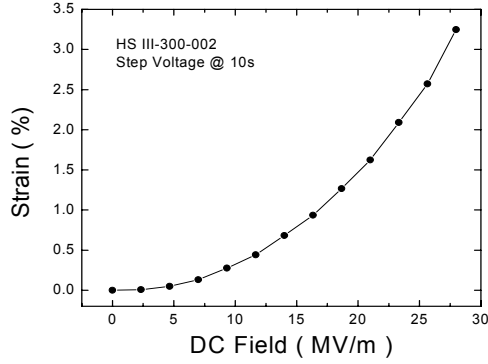


Figure 4. Transverse strain of HS III silicone polymer film as a function of DC field.

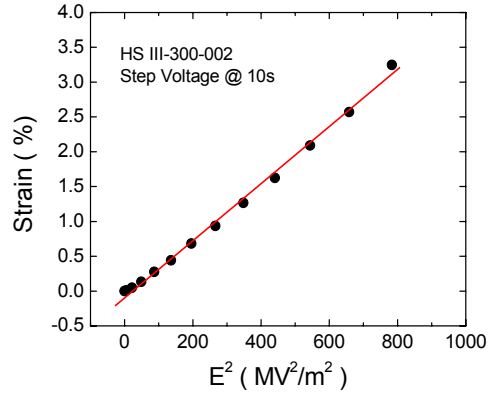


Figure 5. Transverse strain of HS III silicone film as a function of the square of the applied DC field.

strain and may be attributed to creep. Figure 4 shows the strain of HS III silicone film as a function of the amplitude of the step DC electric field. Each value was measured at 10 s after a step field was applied. As seen from the figure, the transverse strain increases with the value of the DC step and a high transverse strain response of 3.25% is observed at a step field of 28.0 MV/m.

For non-piezoelectric silicone polymers, there are two possible effects that contribute to the electric-field induced strain: a Maxwell stress effect and an electrostrictive effect. The Maxwell stress arises from the interaction between free charges on both electrodes (a Coulomb attraction) and it induces a transverse strain, γ , which has approximately the following relationship with the applied field, when the deformation of the film is small (i.e. follows Hooke's law):⁶

$$S = (1 + 2\sigma) \sigma \epsilon_0 \epsilon' E^2 / 2Y \quad (1)$$

where σ is the Poisson's ratio, ϵ_0 is the vacuum dielectric permittivity, ϵ' is the dielectric constant, E is the applied electric field and Y is the Young's modulus. It can be seen from Equation (1) that the transverse strain due to the Maxwell stress is directly proportional to the square of the applied field. On the other hand, the electrostrictive effect is due to the coupling between the polarization and the mechanical response in a material and it is also proportional to the square of the applied field. Separating the contributions of the different mechanisms requires knowledge of other material parameters such as, the elastic compliance, the dielectric constant and the electrostrictive coefficient of the polymer films, but in the dielectric elastomers being studied the electrostrictive contribution is small.⁷ In Figure 5, the data of Figure 4 has been re-plotted to confirm the quadratic dependence of the strain on the applied field.

The dynamic transverse strain of the polymers produced by a sinusoidal electric field has been investigated over a frequency range of 0.01 Hz to 100 Hz. Figure 6 shows a typical transverse elongation of HS III silicone film as a function of time caused by a 1 Hz AC field of 2 kV amplitude. The frequency of the strain response is twice that of the applied field due to the quadratic dependence of elongation on the applied field, as indicated above. Figure 7 shows the dynamic transverse strain of HS III silicone film as a function of the square of AC field at 1 Hz. The dynamic transverse strain increases linearly with the square of the applied AC field as indicated by Equation (1). The maximum strain value measured is 2.08% at a field of 26.3 MV/m, which is smaller than the static strain value (3.25%) at the same amplitude of the electric field as shown in Figure 4. According to Equation (1), the strain responses depend not only on the applied electric field, but also on the dielectric constant. Figure 8 gives the frequency dispersion of dielectric constant of the silicone film over the frequency range from 0.01 Hz to 100 kHz. It can be seen that the dielectric constant decreases with frequency, which leads to a decreasing of strain response as the frequency increases. The frequency dependence of the transverse strain in HS III silicone film is shown in Figure 9. Our results indicate the presence of a resonance around 4 Hz. The resonant frequency is determined by the film sample assembly (the sample, the holder and the platform) under the applied AC field. Disregarding the resonance, the transverse strain generally decreases with frequency as a result of decreasing permittivity and increasing modulus, as predicted by Equation (1).

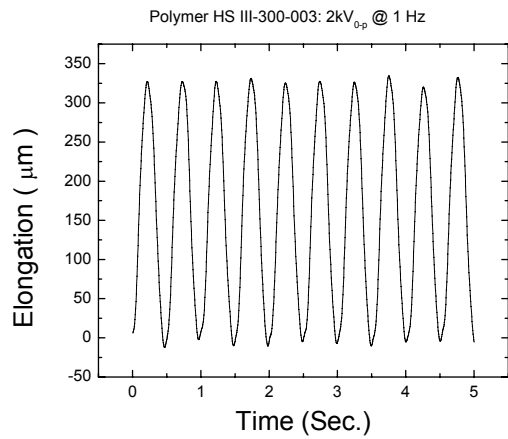


Figure 6. Transverse elongation of HS III silicone polymer film as a function of time.

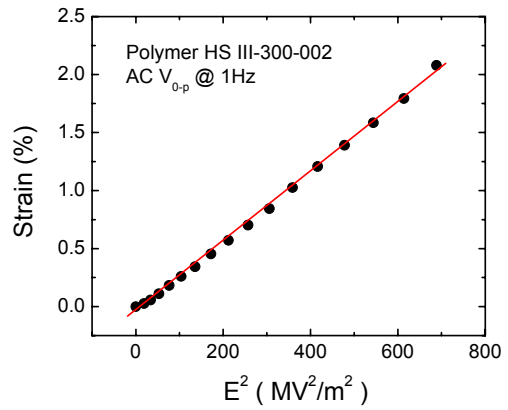


Figure 7. Dynamic transverse strain of HS III silicone polymer film as a function of the square of the AC field.

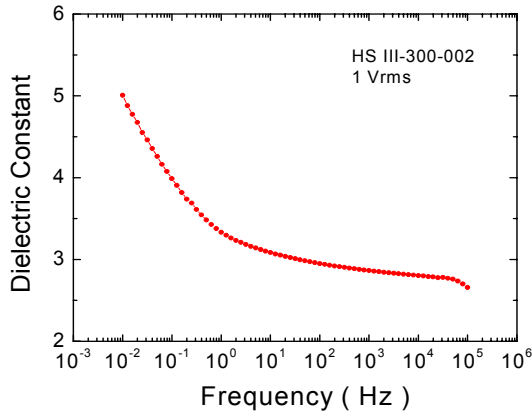


Figure 8. Frequency dependence of dielectric constant of HS III silicone polymer film.

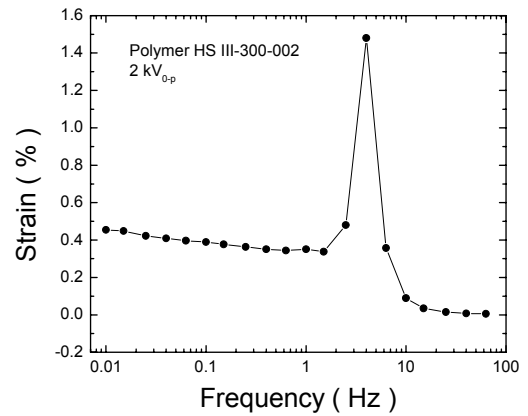


Figure 9. Dynamic transverse strain of HS III silicone polymer film as a function of frequency

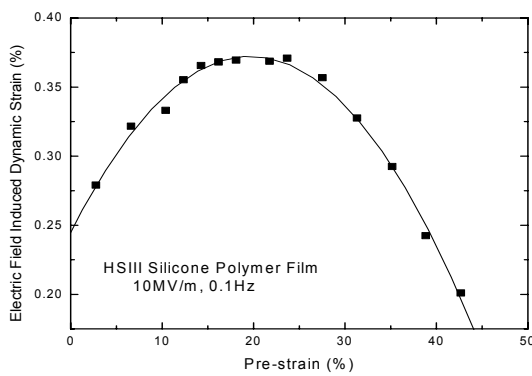


Figure 10. Transverse strain of a HS III silicone polymer film as a function of mechanical pre-strain. Squared points are test data. Solid line is the second order polynomial fitting.

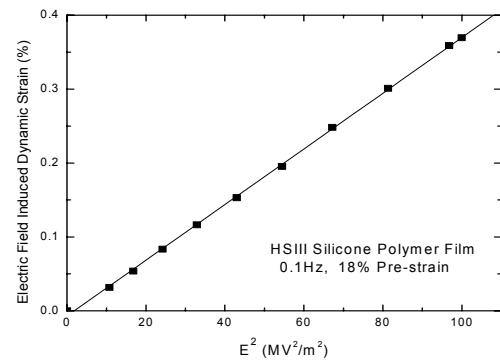


Figure 11. Transverse strain of a HS III silicone polymer film under pre-strain as a function of the square of the applied electric field.

Figure 10 shows the electric-field-induced dynamic transverse strain responses of a HS III silicone polymer film vs. static pre-strain due to mechanical tensile load. The dynamic strain increases initially with the load then decreases after reaching a maximum. Figure 11 shows that although the dynamic transverse strain induced by a given electric field is strongly dependent on the pre-strain, it still depends linearly on the square of the electric field strength under a constant load. Thus, the quadratic relationship between the strain and the driving field remains valid under mechanical loading.

The non-linear behaviour of the strain as a function of pre-strain shown in Figure 10 cannot be understood on the basis of a simple Hooke's law type elastic behaviour that forms the basis of Equation (1) and requires an investigation of more realistic hyperelastic models.

4. HYPERELASTIC MODEL

In hyperelastic theory the material deformation is represented as a stretch ratio, λ_i , instead of the strain, S_i , that is commonly used in linear elastic theory. λ_i is the ratio of final length to initial length in the direction of the i -strain axis, and has the following relationship with the strain:

$$\lambda_i = 1 + S_i \quad (2)$$

where λ_i equals 1 for the un-deformed state. The strain energy density of a hyperelastic material depends on the stretch ratio via one or more of the three invariants, I_i , of the stretch ratio tensor:⁸

$$\begin{aligned} I_1 &= \lambda_1^2 + \lambda_2^2 + \lambda_3^2 \\ I_2 &= (\lambda_1\lambda_2)^2 + (\lambda_2\lambda_3)^2 + (\lambda_3\lambda_1)^2 \\ I_3 &= (\lambda_1\lambda_2\lambda_3)^2 \end{aligned} \quad (3)$$

For an incompressible material:

$$\lambda_1\lambda_2\lambda_3 = 1 \quad (4)$$

so that I_3 equals 1 and does not contribute to the strain energy.

When subjected to an external excitation, the response mode of the film under investigation will depend on its boundary condition. Figure 12 illustrates three special modes of an incompressible isotropic hyperelastic polymer film for which the deformation is relatively simple and easy to analyze. In the case of uniaxial stretching in the length direction, $\lambda_1 = \lambda$, and $\lambda_2 = \lambda_3 = \lambda^{-1/2}$. Here, the suffixes 1, 2, and 3 denote the length, width, and thickness directions, respectively. Another simple situation is the planar (pure shear) stretch. In this mode we have $\lambda_1 = \lambda$, $\lambda_2 = 1$, and $\lambda_3 = \lambda^{-1}$. The third mode is equi-biaxial stretch (inflation), which is equivalent to uniaxial compression where $\lambda_1 = \lambda_2 = \lambda$, and $\lambda_3 = \lambda^{-2}$. For the same stretch ratio in the length direction, the thickness change depends significantly on the stretch mode (Figure 13). Correspondingly, the mechanical stiffness in the thickness direction will also be different.

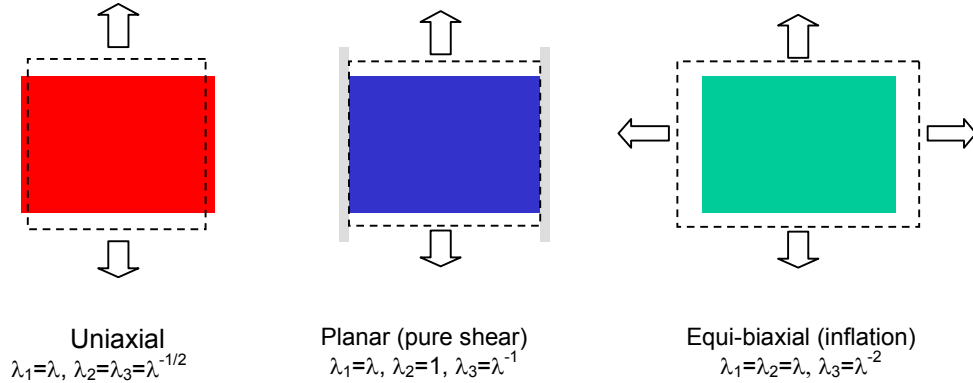


Figure 12. Three particular modes of a polymer film under stretching.

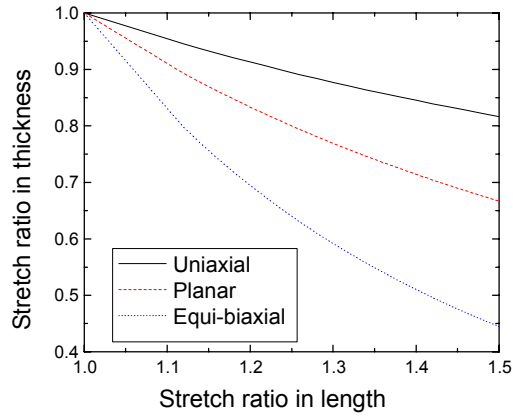


Figure 13. The thickness direction stretch ratios for three modes when the sample has the same stretch ratio in its length direction.

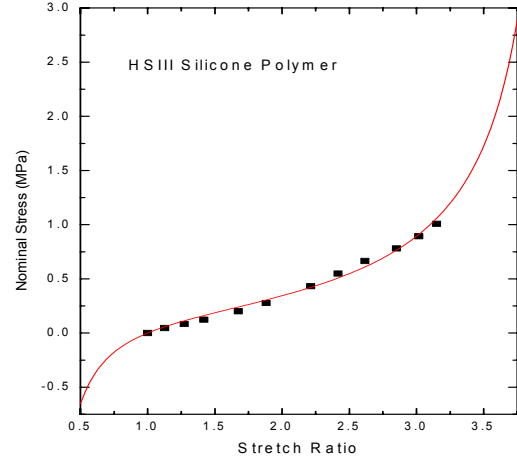


Figure 14. Comparison of stress-strain measurements (dots, with the strain expressed as a stretch ratio) with a curve representing a hyperelastic model, for an HSIII silicone polymer sample.

When an electric field is applied in the thickness direction, the mechanical response is not the same between the different stretch modes although the pre-stretch in length direction of a film caused by a preload is the same. The material is highly nonlinear (hyperelastic). The transverse strain caused by the Maxwell effect will also vary depending on the stretch mode. If the material is not fully covered by the electrode (see Figure 2), the situation will become more complicated. Therefore the actuation produced is not only dependent on the material properties, but is also a function of the actuator structure and the test condition.

Many models have been developed to describe hyperelastic materials.⁹ The Gent model¹⁰ has a very simple form and, in the case of uniaxial stretching of an isotropic material, it can be used to express the nominal stress T_I as

$$T_I = (C/3)(\lambda - \lambda^{-2}) / (1 - J/J_m), \quad (5)$$

where $J^2 = \lambda + 2\lambda^{-1} - 3$. Using Equation (2) and assuming the strain S_I to be very small, Equation (5) can be approximately expressed as

$$T_I = C \cdot S_I, \quad (6)$$

which has the same form as Hooke's law with C being the Young's modulus. This shows that the stress – strain relation of a hyperelastic material can be represented by Hooke's law when the strain is very small, and it explains why the linear elastic model describes the behaviour of the load-free actuator fairly well⁶ given that the deformation due to applied electric field is normally not very large (the highest deformation reported was 3.25%). Figure 14 shows the agreement between our experimental data and Equation (5), which is represented by the continuous line in the figure. The two parameters used for generating the curve representing Equation (5) are 0.6 MPa for the small strain tensile modulus, C , and 25 for the maximum value J_m of the J parameter of the HSIII silicone material. The J_m value of 25, corresponds to a maximum stretch ratio of $\lambda_m = 5$. Both parameters represent the material being investigated reasonably well.

The direct application of the Gent model to understand the behaviour depicted in Figure 10 is complicated by two factors. Firstly, the entire specimen is not covered by the electrodes and therefore the inactive part of the specimen will have a restraining effect and is likely to reduce the observed strain. Secondly, the actual stretch mode of our specimen does not conform to any ideal mode such as those depicted in Figure 12. It is therefore necessary to use finite element modelling to implement Gent's model for our specimen geometry.

5. FINITE ELEMENT ANALYSIS (FEA)

Many hyperelastic models are currently available in commercial finite element software packages. Due to its availability, we have used the Ogden model from the package ANSYS¹¹ as our numerical tool to simulate the actuator functions and details regarding the numerical analysis are to be found elsewhere.¹² The results of the FEA were compared with experimental observations for two types of HSIII silicone specimens: (i) narrow electrode actuators with a regular inactive edge of 20 mm width, and (ii) narrow electrode actuators with a narrower inactive edge of 6 mm width. Figures 15 and 16 show a comparison between our experimental results and our FEA model for the elongation of the electrode and of the whole film due to pre-load. These figures show good agreement between the FEA model and observations of strain under pre-load.

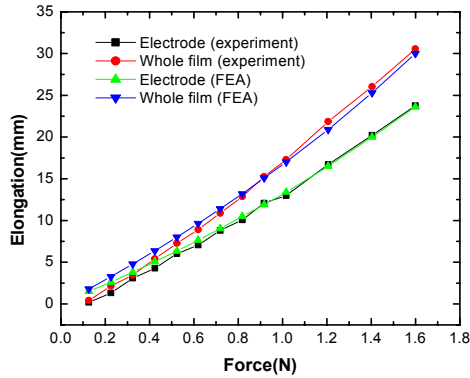


Figure 15. Elongation as a function of pre-load for an HSIII silicone specimen with a regular inactive edge (20 mm)

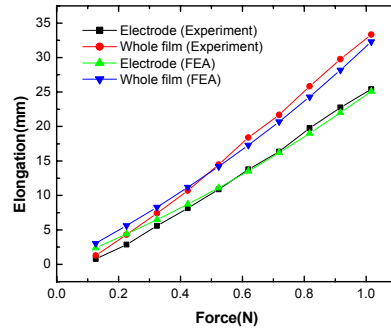


Figure 16. Elongation as a function of pre-load for an HSIII silicone specimen with a narrow inactive edge (6 mm).

The strain produced by the applied electric field is the most important property for a polymer actuator. Figure 17 shows that there is a reasonably good agreement between the FEA results and our experimental measurements for the elongation of an HSIII silicone specimen with a narrow inactive edge as a function of the applied electric field squared. In Figure 18 the FEA model predictions for the electric-field-induced elongation as a function of pre-strain for the HSIII silicone specimen with the narrow inactive edge are compared with our observed values over the full range of applied electric fields. The FEA model does not currently predict any decrease in strain at the higher values of pre-strain as has been observed, although the predictions agree well with observations for pre-strains below about 15%. However the Gent model curve shown in Figure 14 indicates that the elastic modulus goes up non-linearly and sharply both when the elastomer is compressed (as happens in the thickness direction during actuation) and in elongation (as happens in the transverse plane of the actuator). Equation (1) shows that as the elastic modulus, Y , increases, the strain will decrease. This is perhaps a partial explanation for the observed decrease in dynamic strain amplitude under higher pre-strains (Figure 10). Efforts to incorporate the variation of modulus with pre-strain into the FEA model are currently under way.

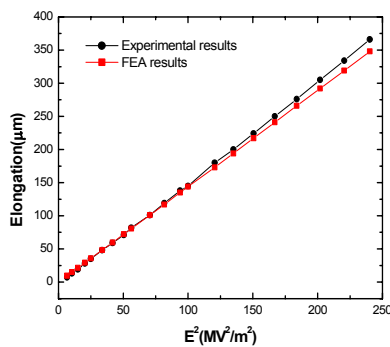


Figure 17. Elongation of an HSIII silicone actuator with a narrow inactive edge as a function of the square of the electric field.

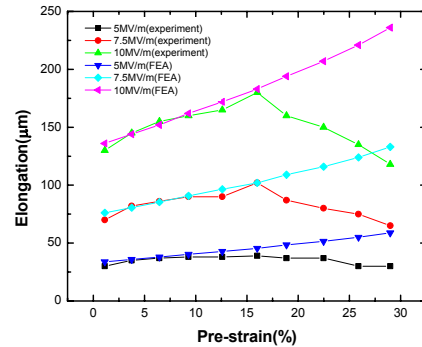


Figure 18. Elongation of the HSIII silicone specimen with the narrow inactive edge as a function of pre-strain: comparison of FEA model predictions with experimental results.

6. CONCLUSION

We have presented the results of an experimental investigation of the transverse strain response of Dow Corning HS III silicone dielectric elastomer actuators. Most of our results can be understood on the basis of Gent's hyperelasticity model and a finite element model that is required to take account of the non-ideal stretch modes involved in the experimental measurements.

ACKNOWLEDGMENTS

Funding support from Defence Research and Development Canada is gratefully acknowledged.

REFERENCES

1. Y. Bar-Cohen, *Electroactive Polymer [EAP] Actuators and Artificial Muscles – Reality, Potential and Challenge*, SPIE Press, Bellingham, WA, 2001.
2. R. Kornbluh, R. Pelrine, Q. Pei, S. Oh, and J. Josef, "Ultrahigh strain response of field actuated elastomeric polymers, *Electroactive Polymer Actuators and Device*, Y. Bar-Cohen, ed., *Proc. SPIE* **3987**, pp. 51-64, 2000.
3. R. E. Pelrine, R.D. Kornbluh and J.P. Joseph, "Electrostriction of polymer dielectrics with compliant electrodes as a means of actuation", *Sensors and Actuator*, **A64**, pp.77-85 1985.
4. Z-Y. Cheng, V. Bharti, T-B. Xu, S. Wang, Q.M. Zhang, T. Ramatowski, F. Tito and R. Ting, , "Transverse strain responses in electrostrictive poly(vinylidene fluoride-trifluoroethylene) films and development of a dilatometer for the measurement" , *J. Appl. Phys.*, **86**, 2208-2214, 1999.
5. W. Ren, G. Yang, B.K. Mukherjee and J.P. Szabo, "Interferometric measurement of the transverse strain response of electroactive polymers", *Electroactive Polymer Actuators and Devices*, Y. Bar-Cohen, ed., *Proc. SPIE* **5385**, pp. 395-405, 2004.
6. W. Ren, B.K. Mukherjee and J.P. Szabo, "The transverse strain response of electroactive polymers measured using a laser Doppler interferometer", *Proc. 6th CanSmart Meeting: Int. Workshop on Smart Materials and Structures*, CanSmart Group Kingston, Canada, 331-342, 2003.
7. Q.M. Zhang, J. Su, C.H. Kim, R. Ting, and R. Capps, "An experimental investigation of electromechanical responses in a polyurethane elastomer", *J. Appl. Phys.*, **81**, 2770-2776, 1997.
8. L. R. G. Treloar, *The Physics of Rubber Elasticity*, Clarendon Press, Oxford, 1975.
9. M. C. Boyce and E.M. Arruda, "Constitutive models of rubber elasticity: A review", *Rubber Che. Technol.* **73**, pp. 504-523 (2000).
10. A. Gent, "A new constitutive relation for rubber", *Rubber Chem. Technol.*, **69**, pp.59-61 (1996).
11. www.ansys.com
12. G. Yang, G. Yao, W. Ren, G. Akhras, J.P. Szabo and B.K. Mukherjee, "The strain response of silicone dielectric elastomer actuators", *Electroactive Polymer Actuators and Devices*, Y. Bar-Cohen, ed., *Proc. SPIE* **5759**, pp. 134-143 (2005).